

## Double-Tuned Hopping-Coil Probe for Dynamic-Angle-Spinning NMR

M. A. EASTMAN, P. J. GRANDINETTI, Y. K. LEE,\* AND A. PINES

*Materials Sciences Division, Lawrence Berkeley Laboratory, 1 Cyclotron Road, and Department of Chemistry, University of California, Berkeley, California 94720*

Received August 30, 1991

A new design for a double-tuned dynamic-angle-spinning (DAS) probe that employs a RF coil wrapped directly around the stator is presented. The increased filling factor of this design and the smaller RF coil result in improved sensitivity and facilitate the incorporation of  $^1\text{H}$  decoupling capabilities. Since the RF coil is reoriented with the spinning sample, the pulse lengths and sensitivity vary as the cosecant of the angle between the RF coil and the external magnetic field. However, this was not found to be a significant impediment to the usage of the probe. As a demonstration of the probe's performance a  $^1\text{H}$ -decoupled  $^{11}\text{B}$  DAS spectrum of boric acid is presented. © 1992 Academic Press, Inc.

The dynamic-angle-spinning (DAS) (1, 2) method of solid-state NMR has proven to be successful at removing anisotropic line broadenings in the spectra of quadrupolar nuclei (3). The method requires an NMR probe capable of changing the angle between the sample spinner axis and the magnetic field direction. For nuclei having first- and second-order broadening, a minimum of two spinner axis angles are required, and the spinner axis must be changed rapidly (typically, in less than about 100 milliseconds) repeatedly during the experiment.

In order to make this technique useful for applications where  $^1\text{H}$  spin decoupling or cross polarization (4) are necessary, such as removal of the anisotropic contributions to the  $^{13}\text{C}$  spectrum from a directly bonded  $^{14}\text{N}$  spin (5), we have developed a double-tuned DAS probe.

The earliest DAS probe design (2) employed a single-tuned coil wrapped around the stator with the RF leads exiting the housing along the hopping axis, where they made electrical contact with static leads connected to the probe tuning circuit. The pressurized air was then delivered through flexible air lines attached to the housing. A second single-tuned design in which the coil axis can be reoriented rapidly and both the coil leads and air supply hoses move when the angle of inclination of the coil axis is changed has been described, but its utility in DAS has not been demonstrated (6).

A more recent design described by Mueller *et al.* (7) delivers the pressurized air along the hopping axis, eliminating the added inertia of the air lines, and employs a large static coil, which surrounds the entire spinning assembly and offers the advantage

\* Graduate Group in Biophysics and the Chemical Biodynamics Laboratory, University of California, Berkeley, California 94720.

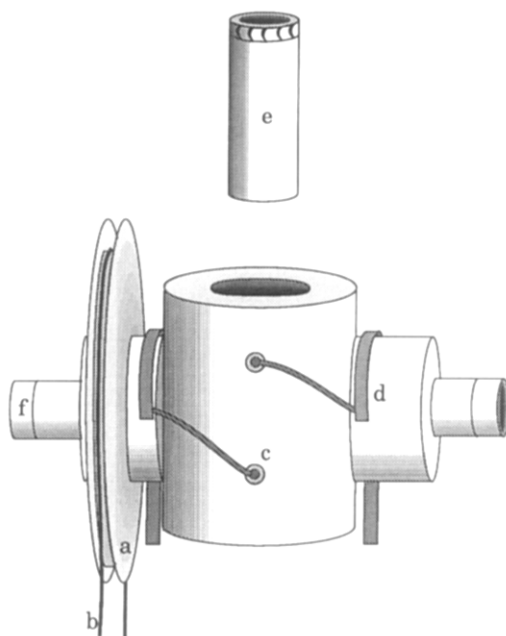


FIG. 1. View of the stator housing (dynamic-angle-spinning assembly). (a) Pulley. (b) Kevlar string connected to motor. (c) Copper pins through which RF coil leads exit the bearing air cavity. (d) Beryllium copper leads connected to capacitors in the double-tuned circuit. (e) Spinner. (f) Ends of stator housing that are held in mounts (not shown) via glass ball bearings.

of equal excitation and detection efficiency at all angles of orientation of the spinning axis. However, this design has limitations with regard to our applications, because the large static RF coil makes it difficult to generate the RF field strengths required for efficient  $^1\text{H}$  decoupling and the low filling factor limits its use for dilute spins systems such as  $^{13}\text{C}$  where sensitivity is important.

Our design, an extension of previous designs from our laboratory (7), utilizes a double-tuned RF coil wrapped around the stator with the pressurized air delivered along the hopping axis. The RF coil is attached to the tuning circuit through moving leads that can withstand the many reorientations required in a DAS experiment while adding negligible inertia to the system.

#### PROBE DESIGN

Following the design of Mueller *et al.* (7), a stator housing containing the sample-spinning apparatus is held between two mounts on glass ball bearing races. High-pressure air for spinning the sample enters the ends of the stator housing through the mounts, with bearing and drive air supplies on opposite ends. On one end of the stator housing is a pulley which is connected via Kevlar string (eight-strand braid obtained from Ashaway Line and Twine, Ashaway, Rhode Island) to an identical pulley attached to a stepper motor (Whedco, Inc., Ann Arbor, Michigan) positioned outside the magnet. An optical encoder (BEI Motion Systems, San Marcos, California) attached to the

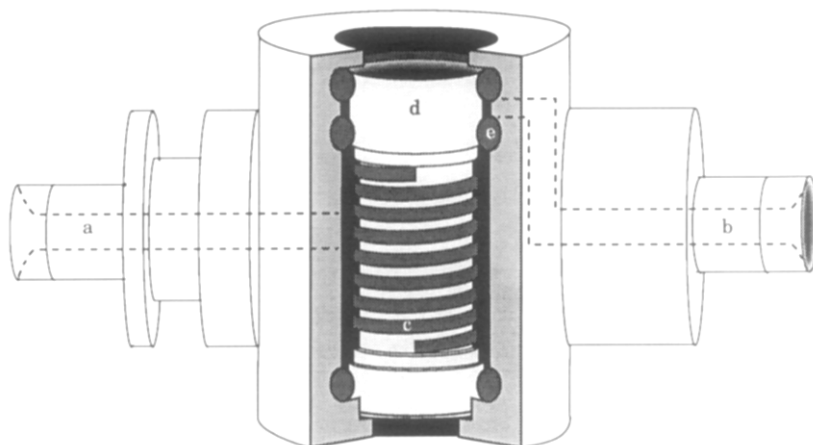


FIG. 2. Cutaway view of the stator housing. (a) Bearing air channel (dotted hidden lines). (b) Drive air channel (dotted hidden lines). (c) RF coil, in bearing air cavity. (d) Stator. (e) O rings separating bearing and drive air supplies.

motor provides feedback to the motor controller to correct for errors in position. With this feedback, the motor can be positioned with an angular resolution of  $0.09^\circ$ . Assuming identical pulleys, the extent to which this resolution is achieved at the sample is determined mainly by the stretching of the Kevlar string and the stick and slip behavior of the bearings.

The stator housing (Figs. 1 and 2) is made of Kel-F and machined in three pieces which are fastened together with pins. The cylindrical central segment holds the stator, a double-bearing zirconia stator manufactured by Doty Scientific Inc. (Columbia, South Carolina) similar to that described elsewhere (8).

The sample RF coil, made of flattened copper wire, is wound around the outside of the stator. After exiting the central segment of the stator housing the leads run to small copper screws on the outer segments of the stator housing (see Fig. 1). Strips of 0.05 mm beryllium copper shim about 3 mm wide and 5 cm in length connect the coil leads at the copper screws to capacitors in the double-tuned circuit (9) mounted

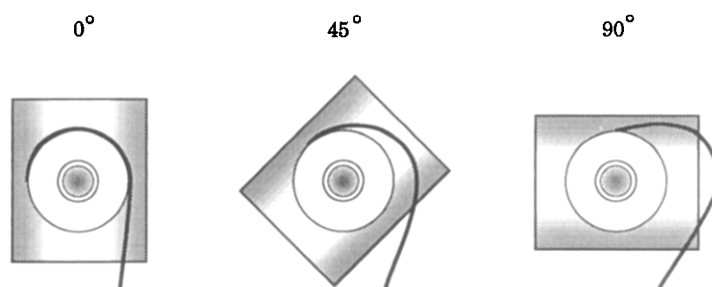


FIG. 3. End-on view of the stator housing, showing the watch spring-like motion of the beryllium copper leads when the angle between the spinning axis and the vertical is varied from  $0^\circ$  to  $90^\circ$ .

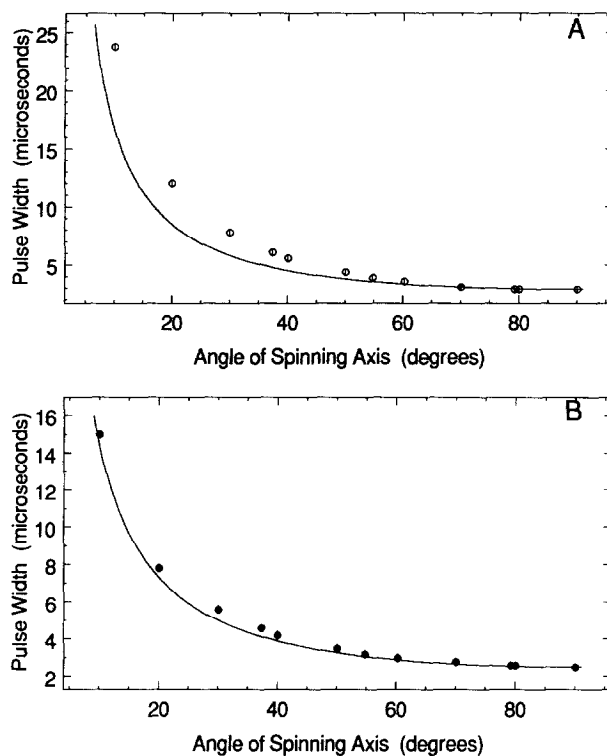


FIG. 4. Experimental and theoretical  $\pi/2$  pulse widths as a function of the angle  $\theta$  between the spinning axis (or the long axis of the RF coil) and the static magnetic field. The sample in each case is liquid boron trifluoride etherate. The magic angle ( $54.7^\circ$ ) was set as described in the text, using KBr. The probe was tuned with the coil perpendicular to the magnetic field, and the solid curve in each plot is  $p(90^\circ)/\sin(\theta)$ , where  $p(90^\circ)$  is the  $\pi/2$  pulse length measured at  $\theta$  equal to  $90^\circ$ . (A) Open circles are pulse widths measured for  $^{11}\text{B}$  with a power input of 184 W. (B) Filled circles are pulse widths measured for  $^1\text{H}$  with a power input of 99 W.

on a circuit board just below the probehead. Figure 3 illustrates the “watch spring” motion of the beryllium copper leads as the spinning axis is changed. We have found that this material and method of attachment distributes the motion of the leads evenly over the lead length during hopping of the stator housing, and is much less prone to breakage than are various configurations of copper wire, braid, or pleated beryllium copper shim.

To protect the leads from strain in the event of an accidental hop to an unreasonable angle, there is a slot in the shape of an arc in the pulley and a peg attached to the end mount. The peg catches the pulley and stops its motion at angles between the vertical and the spinning axis of  $-5^\circ$  and  $95^\circ$ , making angles from  $0^\circ$  to  $90^\circ$  between the static magnetic field and the spinning axis experimentally accessible.

#### PERFORMANCE

Performance tests and experiments were carried out on a homebuilt NMR spectrometer operating at 179.73 MHz for  $^1\text{H}$ .

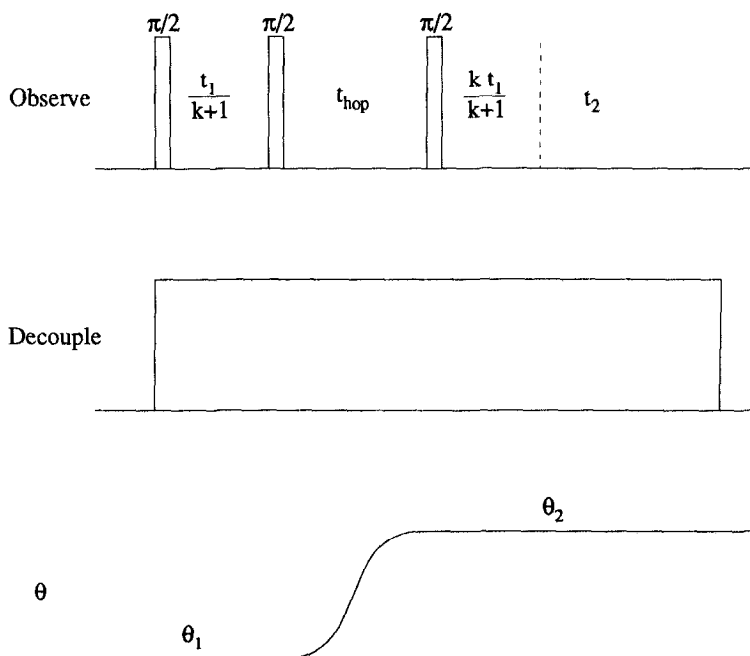


FIG. 5. Pulse sequence for DAS with  $^1\text{H}$  decoupling. The constant  $k$  is determined by the DAS angles  $\theta_1$  and  $\theta_2$  (2). For the experiments presented in this paper  $\theta_1 = 37.4^\circ$  and  $\theta_2 = 79.2^\circ$ .

The magic angle can be located by observing the  $^{81}\text{Br}$  spectrum of  $\text{KBr}$  and stepping the motor to change the angle of the spinning axis. When the rotor is spinning about an axis inclined at the magic angle to the static field a maximum number of rotational echoes is observed. The time,  $t_{\text{hop}}$ , required to change the spinning axis by the amount needed for the DAS experiment (typically about  $40^\circ$ ) can be measured spectroscopically using the  $^{81}\text{Br}$  signal (7). The minimum value of  $t_{\text{hop}}$  is about 25 milliseconds. The angular resolution determined spectroscopically using  $\text{KBr}$  is approximately  $0.5^\circ$ . The bearing air pressure of 40 psi required during a DAS experiment is no greater than for spinning about a single axis (40 psi). Because the beryllium copper leads change position with each hop, their lifetime is shorter than that of other components of the probe. Typically the leads can withstand about three million changes of the spinning axis, equivalent to several DAS experiments, before requiring replacement.

The  $\pi/2$  pulse widths as a function of  $\theta$ , the angle between the coil axis and the external magnetic field, are shown in Fig. 4. These values were obtained after the probe was tuned with the coil axis perpendicular to the external magnetic field. The experimental  $\pi/2$  times are compared with the calculated values  $p(\theta)$  given by the expression

$$p(\theta) = p_m(90^\circ)/\sin(\theta),$$

where  $p_m(90^\circ)$  is the measured  $\pi/2$  pulse width at  $\theta$  equal to  $90^\circ$ . Differences between the calculated and experimental  $\pi/2$  times can be attributed to detuning of the probe

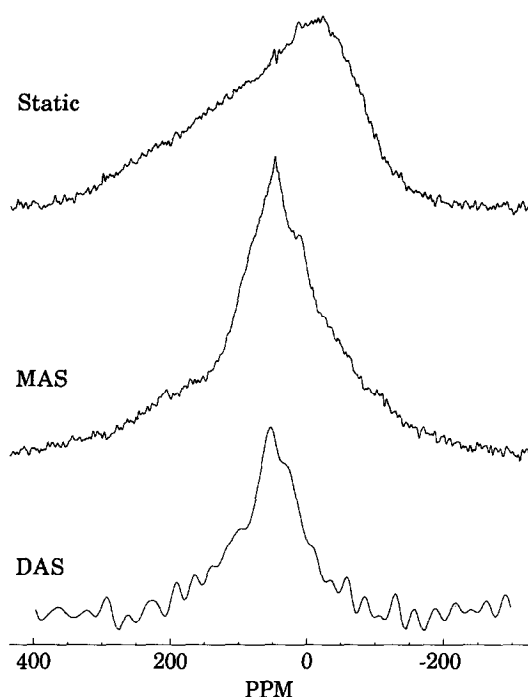


FIG. 6. Static, magic-angle-spinning (MAS), and dynamic-angle-spinning (DAS)  $^{11}\text{B}$  NMR spectra of boric acid ( $\text{H}_3\text{BO}_3$ ) without proton decoupling. Shifts are given in ppm relative to boron trifluoride etherate. For the static and MAS spectra, 512 scans were averaged and 1024 complex points collected with a dwell time of  $16.7 \mu\text{s}$  and delay between scans of 2 s. For the DAS spectrum, 512 points in  $t_2$  and 43  $t_1$  experiments were collected, 1024 scans were averaged for each value of  $t_1$ , and the dwell time in both dimensions was  $25 \mu\text{s}$ . The delay between scans was 1.5 s. The sample-spinning speed for MAS and DAS was 4.9 kHz.

circuit due to changes in the position of the leads and RF coil. The measured pulse widths are reasonably short for both channels for values of  $\theta$  of  $30^\circ$  or greater with RF powers of approximately 100 W on the  $^1\text{H}$  channel and 200 W on the low-frequency channel.

As a demonstration of the utility of the probe in obtaining proton-decoupled DAS spectra for a quadrupolar nucleus, we present  $^{11}\text{B}$  spectra of boric acid ( $\text{H}_3\text{BO}_3$ ). The DAS pulse sequence (2) modified to include  $^1\text{H}$  decoupling is presented in Fig. 5. A reasonable duty cycle is maintained with decoupling continued throughout  $t_{\text{hop}}$ , because  $t_{\text{hop}}$  is of the order of milliseconds. Figure 6 shows the static, MAS, and DAS spectra without proton decoupling. The DAS linewidth is narrower than that for MAS; however, even in the DAS spectrum, the line remains broad due in part to dipolar interactions between  $^{11}\text{B}$  and  $^1\text{H}$ . In contrast, Figure 7 shows the dramatic effect of proton decoupling on the spectra. With decoupling, the MAS spectrum takes a characteristic form reflecting the dependence of the second-order quadrupolar interaction on  $P_4(\cos \theta)$ , the fourth-order Legendre polynomial. The DAS spectrum shows a single line positioned at 69.9 ppm with a width of 461 Hz at half-height. This represents a sevenfold decrease in width from that in the decoupled MAS spectrum and a ninefold decrease

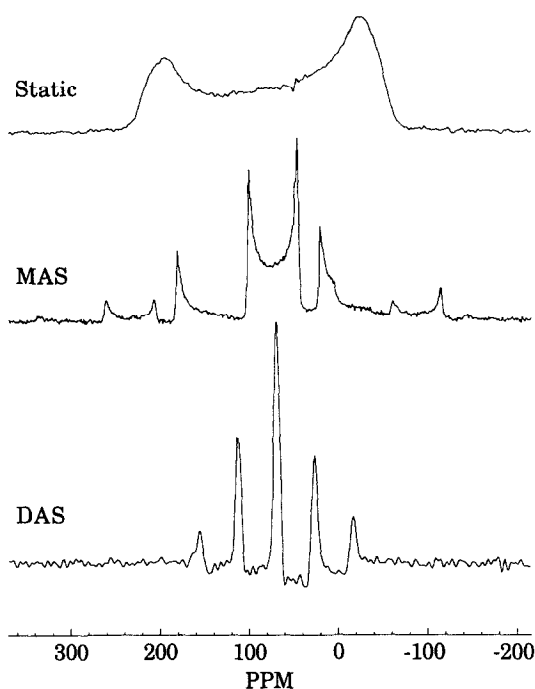


FIG. 7. Static, MAS, and DAS  $^{11}\text{B}$  NMR spectra of boric acid with proton decoupling. Parameters for each spectrum are the same as those for the corresponding spectrum in Fig. 6, except that for the DAS spectrum 119 experiments in  $t_1$  were collected.

from that in the undecoupled DAS spectrum. Figure 8 shows a two-dimensional contour plot of the decoupled DAS spectrum. To distinguish the main line from the spinning sidebands, a second DAS spectrum at a different sample spinning speed was taken (not shown). A recent nuclear quadrupole resonance study using a SQUID detector also revealed only one boron resonance in boric acid (10).

#### SUMMARY

We have developed a double-tuned DAS NMR probe with  $^1\text{H}$  decoupling capability. In addition to  $^1\text{H}$ -decoupled DAS of quadrupolar nuclei, a variety of experiments incorporating  $^1\text{H}$  decoupling, cross polarization, and rapid reorientation of the spinning axis are also practicable. The experiment of Bax *et al.* (11) correlating  $^{13}\text{C}$  chemical-shift anisotropy ( $\theta = 90^\circ$ ) and isotropic chemical-shift frequencies ( $\theta = 54.7^\circ$ ) is one example.

Some advantages of our design over the previous stationary-coil design (7) are the improvement in filling factor and facility of incorporating the  $^1\text{H}$ -decoupling capability due to the smaller RF coil and the ease of inserting and removing the sample spinner. We have demonstrated that alterations in tuning and pulse widths with changes in the angle of orientation of the spinning axis ( $\theta$ ) are not a significant impediment to the usage of the probe. The time required for reorientation of the sample spinning axis is comparable to that observed previously for other designs (2, 7, 6).

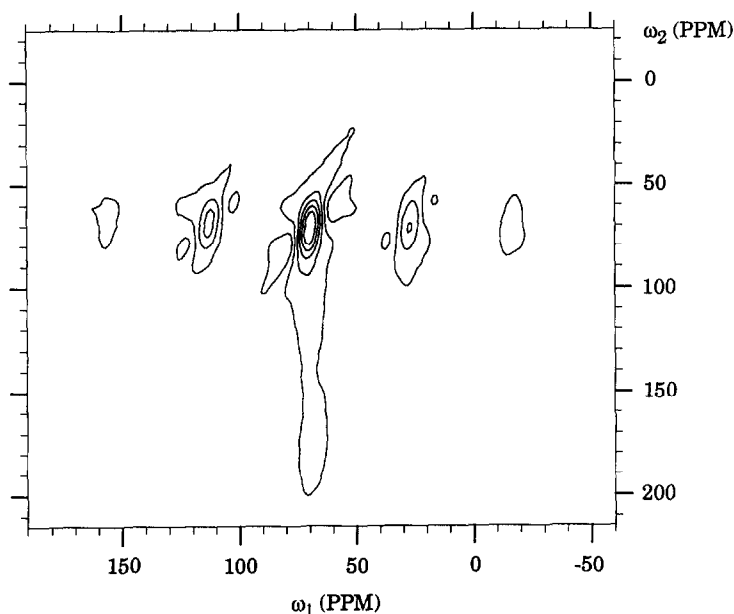


FIG. 8. Two-dimensional contour plot of the  $^1\text{H}$ -decoupled DAS spectrum of boric acid. Shifts are given in ppm relative to boron trifluoride etherate.

One modification of this design, currently in progress, is to replace the RF solenoid coil with a saddle coil or slotted resonator such that the axis of the RF coil is always perpendicular to the static field direction. This modification, which will provide equal excitation and detection efficiency for all angles and retain a relatively high filling factor, will allow us to excite and detect coherences while spinning the sample parallel to the static field. Since spinning a sample about an axis parallel to the external magnetic field is equivalent to not spinning the sample, despite a recent claim to the contrary (12), cross-polarization at  $0^\circ$  can be performed without the difficulties associated with level crossings (13). In addition, this modification permits the use of the  $0^\circ$ ,  $63^\circ$  DAS angle pair, which we have recently found reduces the number of spinning sidebands normally present in a DAS experiment.

#### ACKNOWLEDGMENTS

We thank D. Murai for technical advice and machining the probe and L. Bennett, A. Llor, G. C. Chingas, and K. T. Mueller for helpful discussions. This investigation was supported by the Director, Office of Energy Research, Office of Basic Energy Sciences, Materials Sciences Division, and in part by the Office of Health and Environmental Research, Health Effects Research Division, of the U.S. Department of Energy under Contract DE-AC03-76SF00098. M.A.E. and P.J.G. were supported by National Institutes of Health, National Research Service Awards, F32GM12905-02 and F32GM13626-01, respectively, from the National Institute of General Medical Sciences.

#### REFERENCES

1. A. LLOR AND J. VIRLET, *Chem. Phys. Lett.* **152**, 248 (1988).
2. K. T. MUELLER, B. Q. SUN, G. C. CHINGAS, J. W. ZWANZIGER, T. TERAQ, AND A. PINES, *J. Magn. Reson.* **86**, 470 (1990).

3. K. T. MUELLER, Y. WU, B. F. CHMELKA, J. STEBBINS, AND A. PINES, *J. Am. Chem. Soc.* **113**, 32 (1991).
4. A. PINES, M. G. GIBBY, AND J. S. WAUGH, *J. Chem. Phys.* **59**, 569 (1973).
5. A. NAITO, S. GANAPATHY, AND C. A. MCDOWELL, *J. Magn. Reson.* **48**, 367 (1982).
6. B. C. GERSTEIN, H.-J. PAN, AND M. PRUSKI, *Rev. Sci. Instrum.* **61**, 2699 (1990).
7. K. T. MUELLER, G. C. CHINGAS, AND A. PINES, *Rev. Sci. Instrum.* **62**, 1445 (1991).
8. F. D. DOTY AND P. D. ELLIS, *Rev. Sci. Instrum.* **52**, 1868 (1981).
9. F. D. DOTY, R. R. INNERS, AND P. D. ELLIS, *J. Magn. Reson.* **43**, 399 (1981).
10. C. CONNOR, J. CHANG, AND A. PINES, *J. Chem. Phys.* **93**, 7639 (1990).
11. A. BAX, N. M. SZEVERENYI, AND G. E. MACIEL, *J. Magn. Reson.* **55**, 494 (1983).
12. D.-Y. HAN AND H. KESSEMEIER, *Phys. Rev. Lett.* **67**, 346 (1991).
13. A. J. VEGA, *J. Magn. Reson.* **96**, 50 (1992).